Original Research Paper

IJES *Iranian Journal of Earth Sciences*
*Vol. 13, No. 4, 2021, 266-278.*
DOI: 10.30495/ijes.2021.685394

# Strain geometry and structural analysis of the Oshnavieh ophiolite: A new segment of the Neo-Tethys puzzle

**Majid Niromand, Mahdi Behyari*, Yousef Rahimsouri**

*Department of Geology, Science Faculty, Urmia University, Urmia, Iran*

Received 10 May 2020; accepted 14 September 2020

## Abstract

The closure of the Neo-Tethys ocean associated with the ophiolite obduction and the Oshnavieh ophiolite is the unknown part of the Neo-Tethys suture zone. Three well-known band ratio combinations applied to ASTER satellite image the result shows the ((2+4) /3, (5+7) /6, (7+9) /8) band ratio is the proper combination for the reorganization of rock units in the ophiolite regions. Principal component analysis of the (PC2, PC4 and PC5) is well discriminated against to the rock unit contacts. The general trend of thrust faults is the NW-SE and dip direction is toward the NE. The rake of slickenline on the fault plane is 80°-90° and the mechanism of movement is the pure thrust. The shear sense indicator such as Z-type parasitic folds or mica-fish and S-C fabrics confirm right-lateral shearing sense in the shear zone. Strain geometry on the obducted slab evaluated by the shape of the mineral grains. In the shear zone strain ellipsoid shape is the prolate type and formed under constrictional regime, the Flinn K-value of these samples changes between 2.71 to 11.67 and lode ratio between -0.42 to -0.63. Most of the samples taken from the thrust fault zone located in the flattening zone and strain ellipsoid are pancake-shaped and formed under contractional regime the k-value varied between 0.44 to 0.80 and Lode ratio range is 0.32 to 0.5. The displacement in the thrust zone and shearing by the shear zone disrupted the ophiolite sequence and created an ophiolite mélange.

***Keywords:*** *Ophiolite, ASTER image processing, PCA, Strain geometry, Flinn diagram, NW Iran*

## 1. Introduction

The ophiolites are the remnant parts of the oceanic crust that is obducted onto the edge of the continental plate. The ophiolite units are clues to determination geodynamic evolution in the most orogenic belt and record the evidence of deformation and metamorphism conditions during the obduction (Hassanipak and Ghazi 2000; Khalatbari-Jafari et al. 2004; Moghadam and Stern 2015). Ophiolite rocks also can be the host for the valuable ore deposit like chromite (Rajendran et al. 2012). Therefore, discrimination of the ophiolite terranes in the suture zone is important from several aspects such as geodynamic issue and ore deposition. The Neo-Tethys ophiolites formed through the collision of Arabian plate with Eurasia, coevally with the propagation of the Zagros orogeny from the late cretaceous (Alavi 1991; Khalatbari-Jafari et al. 2003; Mohajjel et al. 2003; Khalatbari-Jafari et al. 2004; Yazdi et al. 2019; Agard et al. 2011; Moghadam and Stern 2015). The Study region is one of the unknown parts of Neo-Tethys ophiolite. The Neo-Tethys suture zone coincides with Main Zagros thrust fault (Agard et al. 2005) and ophiolites have dispersed exposure along this zone (Fig 1a). The Neo-Tethys ophiolites within the Iran Borders based on geographical dispersion divided into four groups and from NW to SE consist of Azerbaijan ophiolites (Maku-Khoy-Salmas), Kurdistan ophiolites (Oshnavieh, Piranshahr, Sardasht), Kermanshah ophiolites (Sahneh, Harsin) and Neyriz ophiolites (Esfandegheh, Haji Abad) (Fig 1b) (Shahabpour 2005; Monsef et al. 2010; Saccani et al. 2013; Behyari et al. 2018).

The Oshnavieh ophiolite is an unknown part of the Neo-Tethys ophiolite and is located between Piranshar and Salmas ophiolites. There has been not performed a systematic investigation of these ophiolites and geodynamic and relation with other ophiolites are not well Study. The Oshnavieh ophiolites mainly consist of serpentinized ultramafic units such as harzburgite and dunite (Fig 1c), that overlaid with gabbro and basalt units. These Rock units mainly consists of clinopyroxene and olivine with plagioclase (Fig 1d) Deformation and faulting (Fig 1e) activity caused to disrupting of the ophiolite sequence and formed the ophiolite mélange. For the discrimination of the members of the ophiolite sequence applied remote sensing technique. The ASTER satellite image bands and longer wavelength regions allow to separate the ultramafic units on the satellite image and provide details lithological maps (Amer et al. 2010; Tangestani et al. 2011; Rajendran et al. 2012). Structures in the Study region affected by the obduction process and have a complex pattern. For the characterizing of the strain geometry on the Oshnavieh ophiolite during emplacement assessed the structures such as foliation, faults, shear zone indicator, and sectional strain data provide from XZ, XY, and YZ plane of samples. In this research, we applied the ASTER satellite image SWIR region after primary image processing to discriminate the ophiolite lithology in the study region.

*Corresponding author.
*E-mail address (es):* m.behyari@urmia.ac.ir

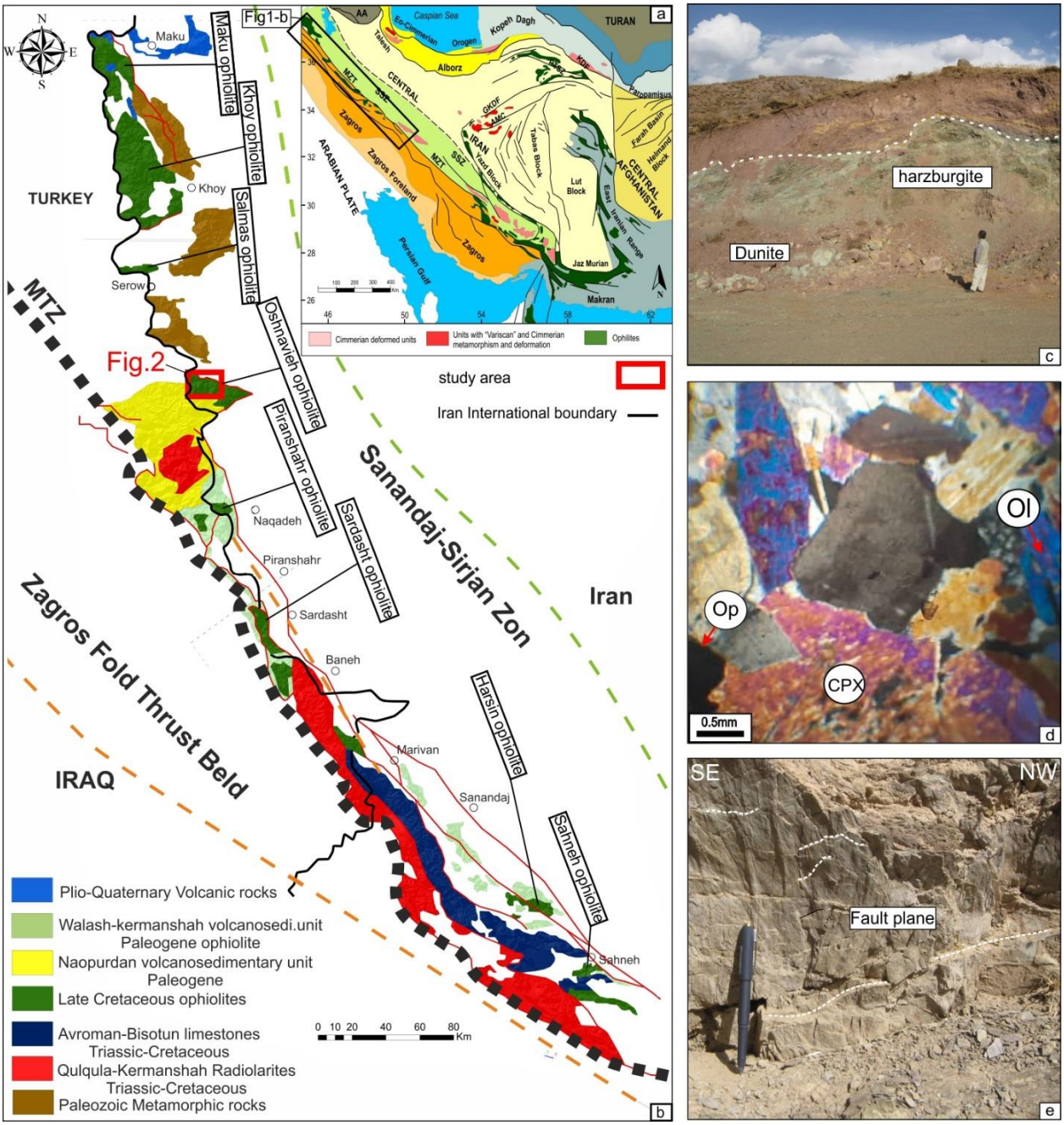


Fig 1. Regional map of the study area. a) major structural zone of Iran. b) The Neo-Tethys Ophiolites distribution along the suture zone in the NW and W Iran Modified after (Moghadam and Stern 2015). c) The ophiolite rock units in the study region consist of altered harzburgite and dunite. d) Thin section of ophiolitic rock, Ol: Olivine, CPX: clinopyroxene, OP: opaque minerals. e) The reverse fault plane within ophiolite unite.

The emplacement of the ophiolite units on the continental crust associated with change in the strain. For evaluating the deformation pattern in the Oshnavieh ophiolite terrene strain ellipsoid shape extracted from available strain markers such as deformed grains shape. The result plotted on the Flinn and HSU diagrams and detected the variation of the strain geometry on the ophiolite slab.

## 2. Geological background

About the age of Neo-Tethys ocean closure is no agreement and remained as a controversial subject in the geodynamic evolution of the Zagros orogeny (Alavi 1994; Mohajjel and Fergusson 2000; Agard et al. 2005; Mahdavi et al. 2015; Sarem et al. 2021). Two assumptions has more adherent some researcher with attention to the geochronologic age of Neo-Tethys

ophiolite (Khalatbari-Jafari et al. 2004) and upper Cretaceous unconformity accepted the late cretaceous for the final oceanic closure e.g. (Berberian and King 1981; Alavi 1994; Mohajjel et al. 2003). But most of the recent research with the attention of the increasing of exhumation rate in the Eocene and Miocene also maximum activity of volcanic arc in Eocene proposed this period for the final collision e.g. (Axen et al. 2001; Ballato et al. 2010; François et al. 2014; Behyari et al. 2017). The continental collision caused to development of the three major structural zones consists of Zagros fold and thrust belt, Sanandaj-Sirjan metamorphic zone and Urmia-Dokhtar magmatic arc (Berberian and King 1981). The suture zone lies along the Zagros main thrust faults and chain of ophiolites dispersed along the suture zone (Fig 1a).

### 2.1. Neo-Tethys ophiolites

The Azerbaijan ophiolites consist of three ophiolite bodies (Salmas -Khoy- Maku) covered area more than 4000 $Km^2$. The mantel lithology in these Ophiolites is lherzolite, harzburgite with minor chromite and crustal lithology comprises of gabbro, pillow to massive lavas and breccia pyroclastic units. The radiometric K-Ar age of the gabbro's revealed 73-101 Ma age (Khalatbari-Jafari et al. 2003; Khalatbari-Jafari et al. 2004; Monsef et al. 2010). In this region ophiolite mostly covered by the late cretaceous to early Paleocene pelagic limestone, radiolarite, turbidities and pyroclastic rocks. The geochemical characterization confirmed Mid-ocean ridge basalt (MORB) type ophiolite and proposed tectonic setting of these ophiolites propagated in the mid-oceanic ridge and back-arc basin, these ophiolites associated with mica schist, phyllite and amphibolite metamorphic rocks (Hassanipak and Ghazi 2000; Khalatbari-Jafari et al. 2003; Khalatbari-Jafari et al. 2004; Monsef et al. 2010; Moghadam and Stern 2015; Behyari et al. 2018).

The Kurdistan ophiolites are less well-known part of the Neo-Tethys ophiolites, this group includes (Oshnavieh, Piranshahr, Sardasht) ophiolites with an area approximately 1000 $km^2$. The Kurdistan ophiolites linked the Zagros ophiolites to Azerbaijan ophiolites. The general trends of this units are NW-SE parallel to Iran-Iraq border and Main Zagros Thrust Fault (MZTF) (Moghadam and Stern 2015) the mantel lithology mainly comprises serpentinized harzburgite, dunite and chromite and crustal lithology is mixing of ultramafic gabbro, diorites, dike, and pillow lava. The Ar-Ar radiometric age of these ophiolites is about 106-92 Ma (Saccani et al. 2014). This ophiolite generally covered by the late cretaceous pelagic limestone and radiolarites and accompanied by Sanandaj- Sirjan zone metamorphism the age of ophiolite assumed late cretaceous (Aswad et al. 2011; Ali et al. 2013; Saccani et al. 2014; Moghadam and Stern 2015).

The Kermanshah ophiolite constituted diverse rock units such as lherzolite, harzburgite, dunite and gabbros, the radiometric dating revealed two ophiolites in this region the older unit is 222Ma and younger unite 86 Ma (K-Ar) and 98 Ma (U-Pb) (Saccani et al. 2013). The older ophiolite overlaid by Triassic to Cretaceous Bistun limestone and Kermanshah Radiolarite and younger unit covered by the late-cretaceous pelagic limestone, radiolarites, and turbidites. The older ophiolite tectonic setting proposed late Permian Triassic continental rifting and younger ophiolite arc (Saccani et al. 2013; Moghadam and Stern 2015).

The Neyriz ophiolite is mélange of peridotite, dunite, sheeted dikes and pillow lavas. Ar-Ar dating indicated 92-93 Ma age of this unit (Babaie et al. 2006; Shafaii Moghadam and Stern 2011). The Neyriz ophiolite covered by the pelagic limestone and Radiolarite, with attention geochemical characterization of this ophiolite is the subduction zone type ophiolite and formed in the infant arc tectonic setting (Shahabpour 2005; Babaie et al. 2006; Sarkarinejad et al. 2009; Shafaii Moghadam and Stern 2011; Moghadam and Stern 2015).

### 2.2. Oshnavieh ophiolites

The Oshnavieh ophiolite is a member of Kurdistan ophiolites and linked the Kermanshah ophiolite to the khoy- salmas ophiolites on the suture zone. The emplacement mechanism of the Oshnavieh ophiolite massifs onto the Iranian microcontinent and structural evolution is completely unknown but few studies have been done on clarifying the igneous evolution of this region (Aswad et al. 2011; Ali et al. 2013; Saccani et al. 2014). In detail, the Oshnavieh ophiolite is a 400 square kilometer slab of the Neo-Tethys oceanic crust. This unite is an assemblage of strongly sheared serpentinized ultramafic rocks such as harzburgite, dunite, pelagic limestone, and radiolarite. Diorite and granodiorite intruded in the ophiolite unit and metamorphosed the host rocks, this contact metamorphism has small exposure in the Study district. The evidence of regional dynamo-thermal metamorphism such as penetrative foliation also documented in this region this event cause to accommodation of deformation in the mylonitic zone (Sarkarinejad et al. 2008; Sarkarinejad et al. 2009), the kinematic characteristics of this event explained in the kinematic evolution section. The basalt with porphyric fabric is another major rock unit in this area, the plagioclase altered to sericite and chlorite and clay minerals and clinopyroxene altered to chlorite and serpentine. The serpentized ultramafic rocks have a dispersed exposure within ophiolite unit. In the thin section, major mineral is the fine grains serpentine. The segments of the ophiolite unite are generally separated by the NW_SE striking thrust fault.

## 3. Methodology

### 3.1. Remote sensing

The remote sensing is the common methods for mapping of the hydrothermally altered regions (Rajendran et al. 2012). In the Oshnavieh region for the mapping of the ophiolites, exposure applied the ASTER satellite image,

the ASTER is a multispectral imaging system that launched in 1999 (Rowan et al. 2003). The ASTER has 14 spectral bands in the three regions (VNIR, SWIR, TIR), in this contribution applied ASTER SWIR region because of the proper capability of these bands in the surface lithological mapping. The reflectance and absorption of rocks controlled by the mineralogy that covered the surface of rocks. These minerals possible belong to the primary mineralogy phase of ophiolite rocks such as pyroxene, olivine, plagioclase or secondary minerals include sericite, chlorite, clay minerals and serpentine that formed by the alteration process. By the remote sensing and analyzing of reflectance and absorption wavelength discriminate the lithologies. The spectral reflectance of the major minerals in the ophiolite rocks discussed in several earlier research works e.g. (Hunt et al. 1974; Abrams et al. 1988; Cloutis et al. 2004; Rajendran et al. 2012). Standard spectral reflectance detecting by the experimental methods for fresh and altered rocks (Rajendran et al. 2012).

The band rationing and principal component analysis technique used for the mapping of Oshnavieh ophiolite. The band ratio methods have been used frequently to the lithological mapping. In this technique with regarding the spectral signature of the index minerals in the ophiolite units such as serpentinite and harzburgite detected the best combination ratio for the discrimination of the rocks unit. Reflection spectral of the vegetation it my similar to the serpentinite therefore vegetation masked from raw image. In the earlier studies for the mapping of ophiolites rock unit tested some of the ASTER band ratio combination instance (4/7, 4/1, 2/3*4/3) and (4/7, 3/4, 2/1) give acceptable result for mapping of ophiolite terrene (Amer et al. 2010; Rajendran et al. 2012). In the Oshnavieh region also applied these combinations for mapping of the ophiolite. For the separation of the ophiolite ultramafic unit from granite intrusion tested ((2+4)/3, (5+7)/6, (7+9)/8) band rationing (Amer et al. 2010).

PCA is the other technique applied for the mapping of the ophiolite in the Study region. In the PCA methods enhanced spectral reflectance of the target minerals by the decreasing of the irradiation effect in the spectral bands. The eigenvector matrix provides the information about spectral of target minerals and numeric value, this matrix used for detecting principal component to discrimination of the ophiolite units. Major part of spectral information acquiring in the PC (1, 2 and 3) for this in the most of lithological mapping these applied components. The higher order components (4, 5, 6 and 7) combination with lower order can provide valuable data about the target minerals in the image (Amer et al. 2010; Tangestani et al. 2011; Rajendran et al. 2012).

### 3.2. Structural and kinematic evolution

Our study focused on the kinematic analysis, strain geometry and deformation that accompanied by the ophiolite obduction. The deformation distribution is non-uniform in the Zagros collision zone that this variation of the strain geometry imply to the changes in the deformation conditions during the closure of the Neo-Tethys and thrusting of the oceanic crust on the continental edge (Keshavarz and Faghih 2020). The shape of strain ellipsoid or ellipse is the proper technique for the evaluation of strain geometry in the structural geology. Different methods applied to compute of strain geometry in 2D or 3D (Ramsay and Graham 1970; Bhattacharyya and Hudleston 2001; Sarkarinejad 2007; Lisle 2010; Behyari and Shahbazi 2019), the selective methods depended on the deformation conditions such as temperature and pressure, strain markers shape and distribution, mineralogy and the scale of the study. (Watts and Williams 1983; Vitale and Mazzoli 2010; Ring et al. 2015; Behyari and Kanabi 2019). In the Oshnavieh ophiolite deformation associated with the changes in grains shape, for this shape of the grain selected as a marker to the evolution of the strain geometry. For the calculation of strain shape ellipse in 2D, we applied only XZ plane data (normal to the foliation and parallel to lineation). However for the 3D analysis, the samples cut in the three perpendicular planes. In this geometry the grain shape analyzed in XZ plane, XY plane (foliation plane) and YZ plane (normal to the foliation and lineation). The deformed quartz, mica and plagioclase aspect ratio (long axes ratio to the short axes) measured for the extracting of strain ellipsoid shape (Mookerjee and Fortescue 2016). This approach to the calculation of the strain ellipsoid shape associated with uncertainty, for instance maybe measurement performed in the grains with different mineralogical axes or maybe thin section oriented obliquely to the long axes of minerals. We assumed the stretching axes of grains are parallel to the C axes of the minerals this assumption proved by some experimental research (Stallard and Shelley 1995). Despite these uncertainties the calculated strain shape gives speculation of strain variation and deformation conditions in the Study area (Behyari and Shahbazi 2019). Detailed structural and kinematic analysis on the Oshnavieh ophiolite region revealed two types of the structures are dominated, the first set are the successive thrust array sheets and second is the shear zones.

## 4. Results and discussion

Thrust faults in the study area are parallel to the main Zagros thrust (MZT) and resting ophiolite unit on top of the Precambrian basement also stacking ophiolite unit on each other and caused to thickening and mélange of this unit. The exhumation of Precambrian unit in the footwall and over thrust of the Oshnavieh ophiolite on hangingwall indicated that thrust faults in this region are deeply rooted (Agard et al. 2005). The kinematic indicator such as shear sense indicator and stretching lineation revealed transportation direction on the thrust sheets is toward SW and thrust faults are generally dipped to the NE, also subsidiary thrust faults with opposite vergence formed between the major thrust.

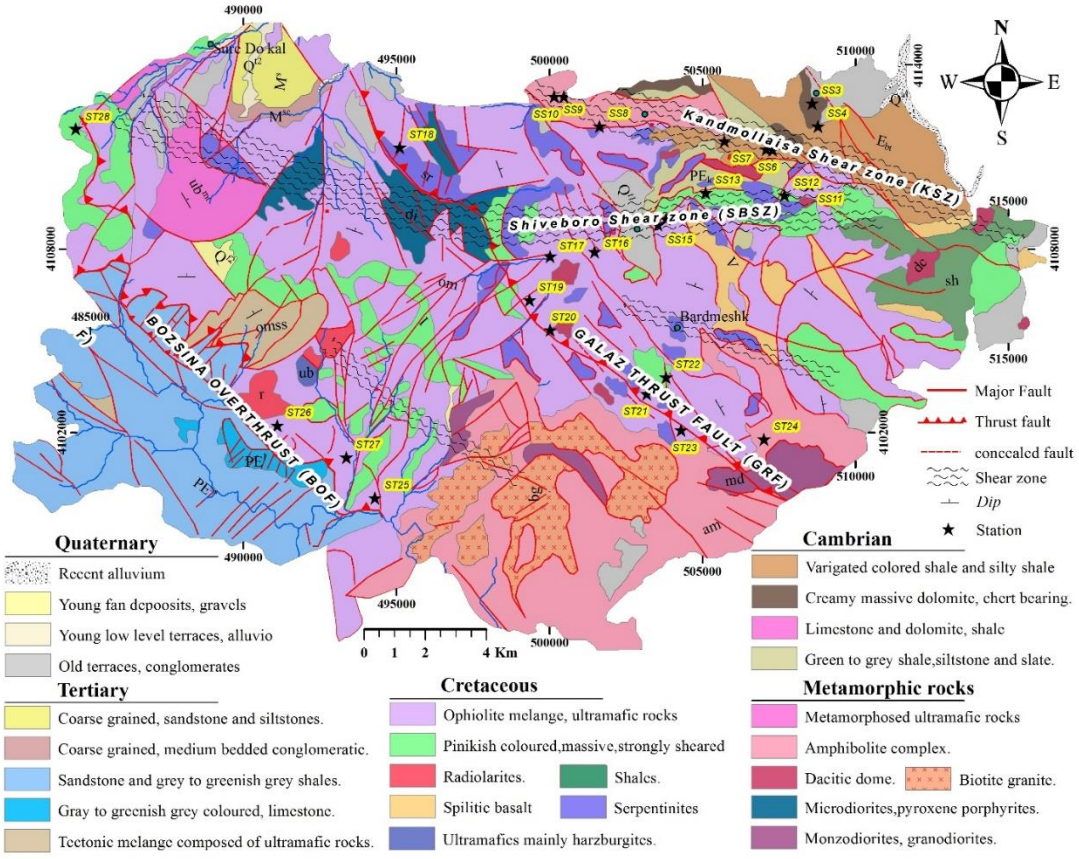


Fig 2. The Geological Map of the Oshnavieh Ophiolite, spatial orientation of the shear zones; Structural stations. The sampling stations shows by yellow color box. ST: Thrust fault samples, SS: Shear zones samples.

Two prominent of this type of faults in the Study region from SW to the NE are Bozsina overthrust fault (BOF) and Galaz reverse fault (GRF). The thrust faults dip increasing from SW to NE on the cross-section (Fig 2).

### 4.1. Major shear zones deformation

The BOF is the low angle over thrust fault near the Iran and Iraq border. The Oshnavieh ophiolitic mélange on the hanging wall thrust on the Precambrian basement in the footwall. There is a lot of change in the strike of BOF but the general trend of this fault is the NW-SE. Ophiolite rock unites lay between BOF and GRF intensively deformed by displacement of fault plane. The general dip of these subsidiary thrusts fault varied between 30° to 45° and dip direction are mostly toward NE. A few back thrust with opposite vergence of general faults formed in this region.

The GRF is the high angle reverse fault within Oshnavieh ophiolite rock units. This fault strike is parallel to the BOF and the dip of the fault plane is approximately 60° to the NE. The fault zone increased permeability of the rock units. Circulation of hydrothermal fluid caused to serpentinization of ultramafic rocks. These serpentinized zone act as indictor for detecting of the faulted area. The fractures are highly concentered in the fault zone and mostly field by the quartz or calcite grains.

The second set of the important structure in the evolution of the Study area is the mylonitic ductile shear zone. The shear zone general trend is the ESE-WNW, and ductile structure such as S-C fabrics, Mica fishes, mylonitic foliation and rotated porphyroblast developed in these zones. The Shiveboro shear zone (SBSZ) and kandmollaisa shear zone (KSZ) is two major zones in the ophiolite zone, these shear zone cut the earlier structures (Fig 2).

The SBSZ is located between the amphibolite and ophiolite unit. The ductile structure is dominated and mostly comprises mylonitic foliation (Fig 3a) in the micro-scale and parasitic folds in the both micro and outcrop scale. Z-type parasitic folds and mica fish imply to the right-lateral shear direction in this zone (Fig 3b). The foliation plane general strike is N30W/50 NE and mostly foliation plane cut by the Fractures (Fig 4a). The quartz grain strongly recrystallized and developed a preferred orientation. In the deformation conditions strain localization in the grain boundary caused to crystal with low dislocation density bulge into crystal with high dislocation density. This process led to recrystallization of fine and independent crystal on grain boundary this process is known as bulging mechanism (Passchier and Trouw 1996).

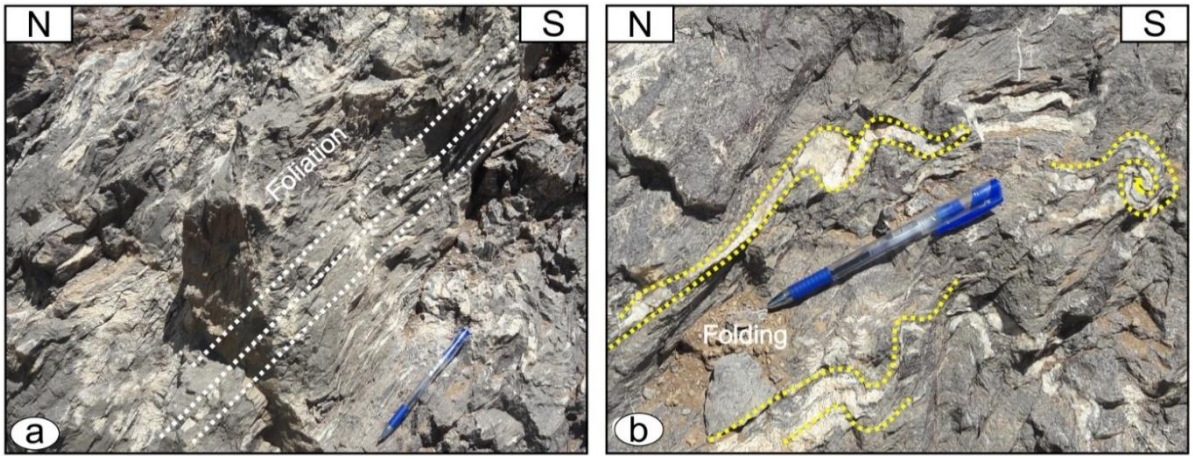


Fig 3. Structures that developed in the SBSZ a) Mylonitic shear zone in the SBSZ. b) Z-type parasitic folds formed as a result of the right-lateral shear zone.

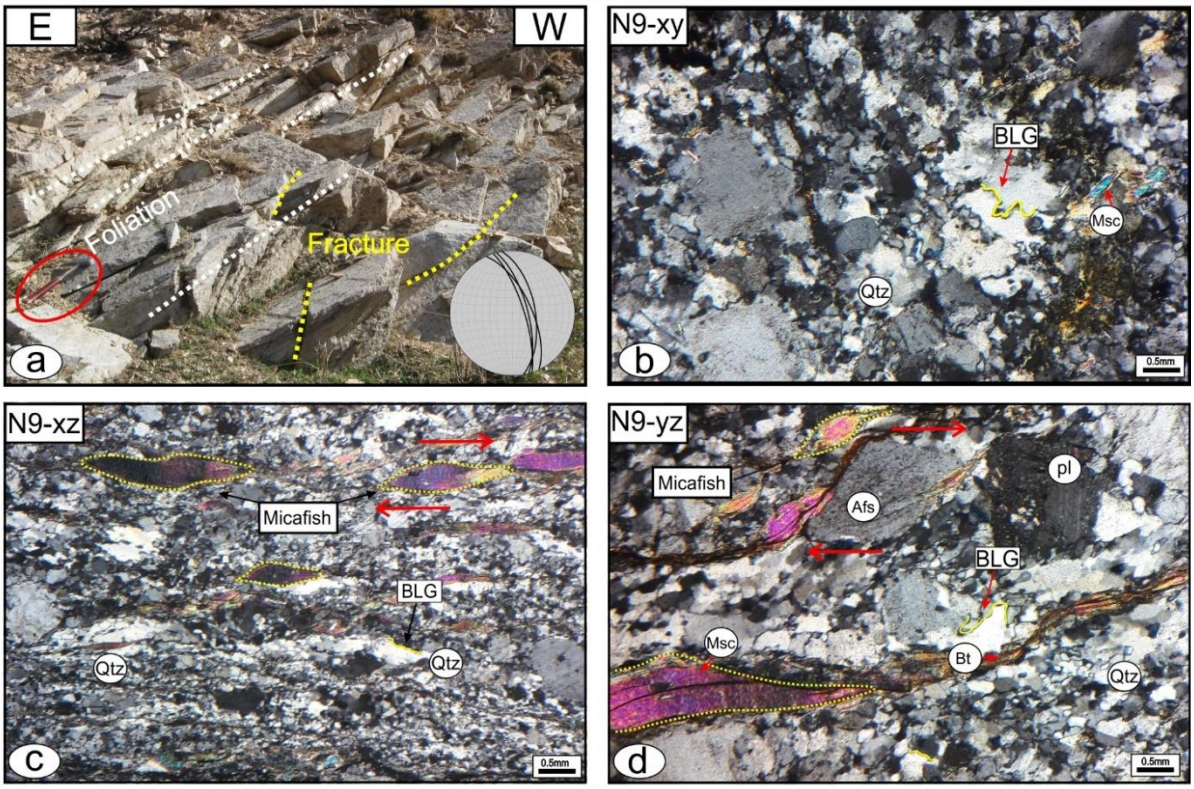


Fig 4. a) Development of the foliation and fractures in the SBSZ. b) Dynamically recrystallization quartz grains in the shear zone, the most frequent recrystallization mechanism in the quartz grains is the bulging. c) Spaced foliation development in the shear zone the cleavage domain is the mica-rich zone and microlithon is the quartz-rich. d) Shearing of mica and alkali feldspar and development of the minerals fish with right-lateral shearing direction. Quartz (Qz), Muscovite (Msc), Alkali feldspar (Afs), Biotite (Bt).

This microstructure developed in the margin of quartz grain (Fig 4b) and micas grain completely stretched and sheared. The mylonitic foliation characterized by the spaced foliation. The cleavage domain consists of mica and Microlithon includes flattened quartz grains (Fig 4c). The Mica and alkali feldspar grains completely sheared and formed fish type structures these minerals fish also confirm the right-lateral shearing direction in the SBSZ (Fig 4d). The KSZ is the NW-SE trending shear zone that developed in the massive dolomitic limestone with the frequent white chert layers (Fig 5a). In the KSZ mylonitic foliation is dominate structures. In this zone Z-type asymmetrical fold revealed right-lateral shearing component. Quartz grain completely recrystallized and are very fine grains and slaty cleavage formed. On the rock slab shear band cleavage is recognizable, the alternation of light and dark layer coincide to C-plane that cut and linked by the S-plane.

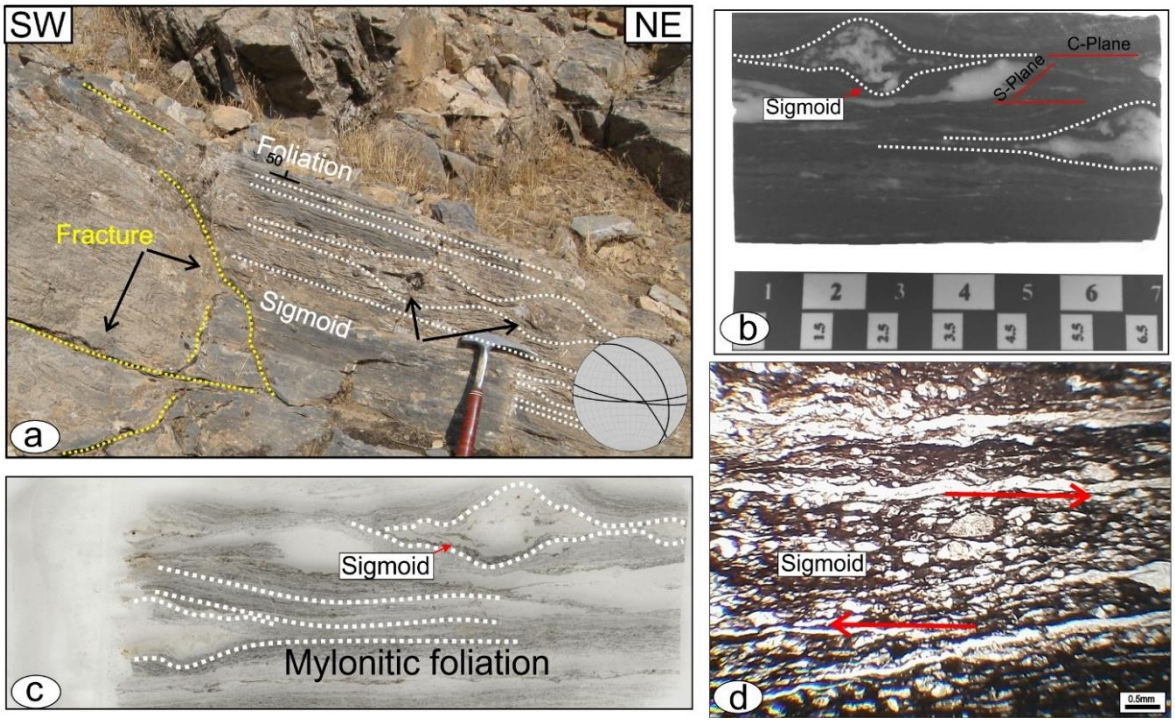


Fig 5. a) The mylonitic foliation in the KSZ. b) The foliation of dark and light grains is associated with the development of the S-C fabrics and sigmoid. c) Sigmoid and mylonitic foliation under right-lateral shearing direction. d) The mylonitic foliation in the shear zone and concentration opaque minerals in the foliated plane as a result of volume loss.

Also that approved the right-lateral shearing direction (Fig 5b). Under shearing conditions sigmoid structure also developed between mylonitic foliation (Fig 5c). In the cleavage domain, the high concentration of the opaque's minerals implies the pressure solution during shearing and contraction in the shear zone (Fig 5d). This evidence indicated deformation in this zone accompanied by the volume change. The ptygmatic folds in this zone and folding with flexural flow indicated the high-temperature deformation in this zone.

### 4.2. Deformation elipsoide

In the two sets of samples strain analysis conducted only in the XZ-plane and in two dimensions, the first group is the sample with high fracture density that preparation of three perpendicular planes for the thin section study was impossible. Second is samples with evidence of volume change during deformation. In these types of the samples strain geometry specifying only in the XZ-Plane and in two-dimensions. In the other samples strain ellipsoid shape derived from the data of XZ-XY and YZ plane and strain analyzed in 3D.

25 oriented samples Study in Oshnavieh ophiolitic rocks. Totally 12 samples analysis in 3D, Samples taken from shear zone labeled as (SSn) and samples taken from thrust zone named as (TSn), other remnant sample analysis in 2D and only on XZ-plane. The best fit ellipse has been drawn for the deformed grains then measured long and short axes of these ellipses. This data applied to evaluate of strain geometry in the Oshnavieh ophiolite slab (Fig 6).

| Sample Name | Long Axis / Short Axis / R | Thin section | Grains Shape | Strain ellipsoied |
|---|---|---|---|---|
| TS27 | 339.168 / 204.39 / 1.662 |  | 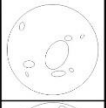 |  |
| TS19 | 336.300 / 221.951 / 1.515 | 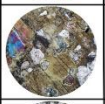 | 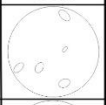 |  |
| TS23 | 157.056 / 91.385 / 1.718 |  | 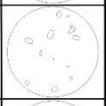 |  |
| Ts26 | 208.596 / 105.672 / 1.973 | 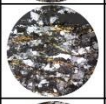 |  |  |
| SS4 | 158.788 / 91.075 / 1.743 |  | 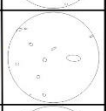 |  |
| Ss9 | 97.760 / 56.703 / 1.724 |  | 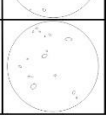 |  |

Fig 6. The parameters applied for the strain ellipsoids in the ophiolite. Long axis and short axis calculated from selected grains.

### 4.3. Relationships of minerals and deformation zones

The discrimination of the ophiolite rock unit and deformation mechanism is critical to the geodynamic interpretation of the collision zone (Hassanipak and Ghazi 2000; Khalatbari-Jafari et al. 2004; Babaie et al. 2006; Saccani et al. 2014; Moghadam and Stern 2015).

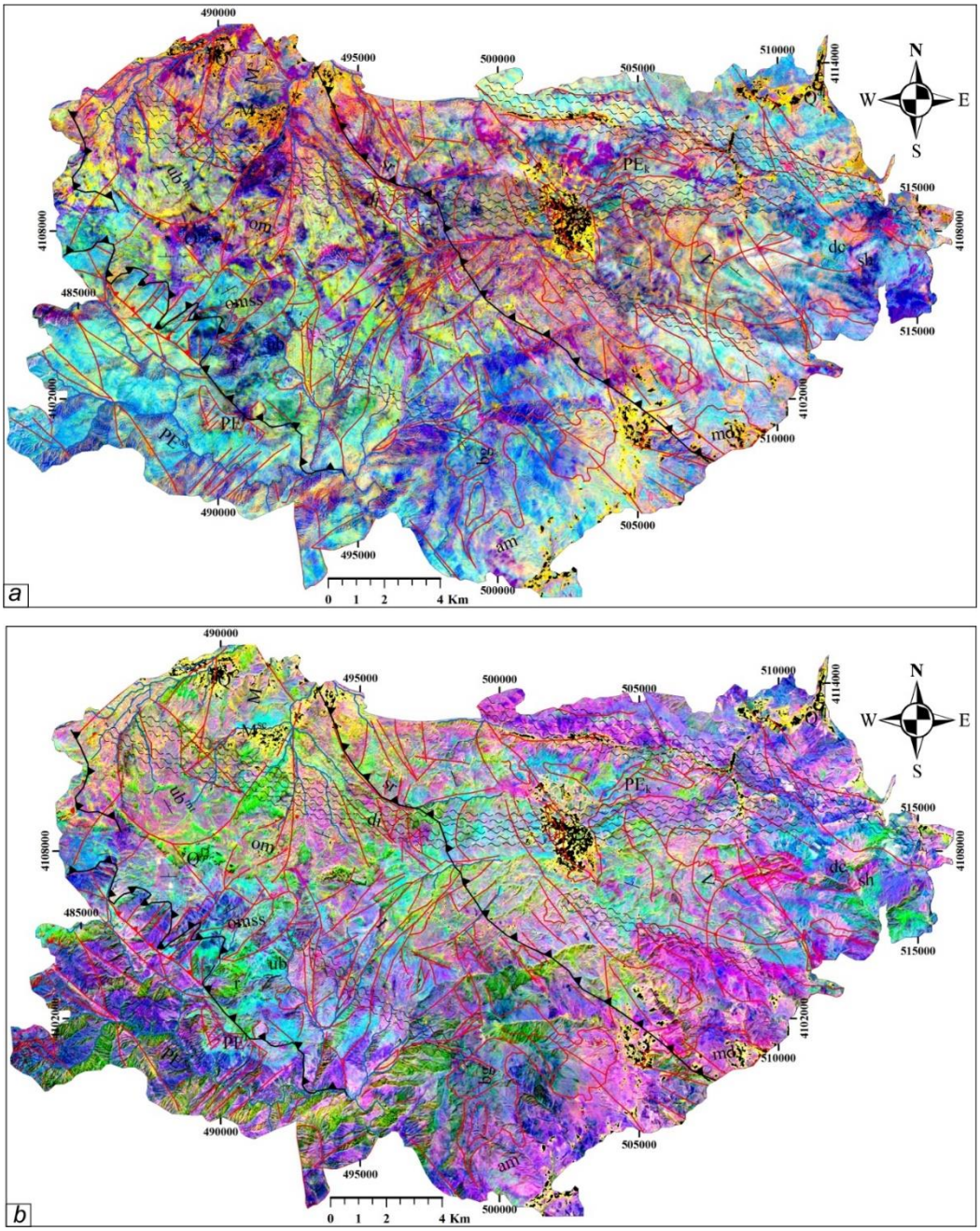


Fig 7. The ASTER RGB band ratio image for discrimination of the ophiolite rock unite. a, b) combination of the (4/7, 4/1, 2/3*4/3) and (4/7, 3/4, 2/1) band ratio (Abdeen et al. 2001).

Neo-Tethys ophiolite doesn't have contiguous exposure on the suture zone and dispersed along the collision zone, the age and mechanism of obduction are not the same in the all ophiolite segment and in some case have confliction with each other (Moghadam and Stern 2015), therefore increasing of ophiolite terrane detection lead to the ascending of the knowledge about the geodynamic evolution of the collision zone. The conducted satellite image processing revealed in the band rationing (4/7, 4/1, 2/3*4/3) the ophiolite mélange the serpentinized ultramafic unit and harzburgite as shown in brown to pinkish colors (Fig 7a). In the band ratio (4/7, 3/4, 2/1) the Precambrian and Cambrian schist and shale are well discriminated by the blue color and the contact between ophiolite unit and surrounding rock units discriminated in green color (Fig 7b).

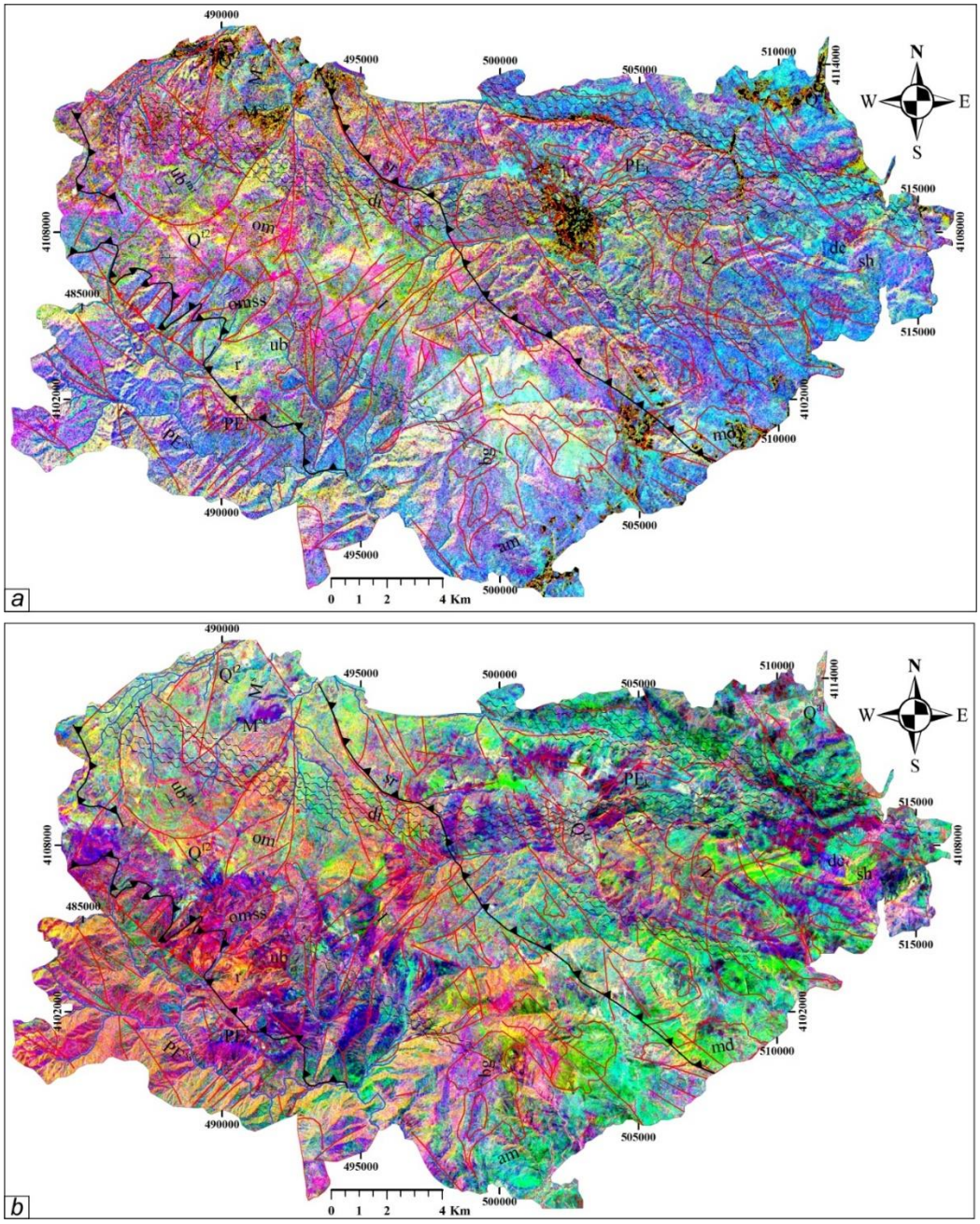


Fig 8. The ASTER RGB band ratio image for discrimination of the ophiolite rock unite a) The band ratio ((2+4)/3, (5+7)/6, (7+9)/8) serpentinites, harzburgite, and metabasalts and intrusions (Amer et al. 2010).b) The RGB image of principal component analysis (PC5, PC4, and PC2).

An ASTER band ratio ((2+4)/3, (5+7)/6, (7+9)/8) applied in the recent researches (Amer et al. 2010; Rajendran et al. 2012) for the mapping of ophiolites (serpentinites, harzburgite, and metabasalts and intrusions). The ASTER image processed by this ratio indicated the biotite granite units (bg) in turquoise blue. Ophiolite unit shows in brown to pinkish colors. The schist and shale with limestone depicted by the blue color on the image and metamorphosed units in the NW of the study region indicated by the brown to orange colors (Fig 8a). In this image, the ophiolite rock unites well discriminated by the boundary of between unit is not clear. In the principal component analysis of ASTER for discrimination of ophiolite units focused on the three PC (PC2, PC4 and PC 5) and produced an RGB image, in this image PC2 assigned for the red channel, PC4 for green channel and PC5 to the blue channel. The resulted image shows the Precambrian schist and shale with orange colors in the SW of the Study region. Harzburgite and serpentine shows by the green and turquoise blue in the central part and basic gabbro in the blue color (Fig 8b).

The image processing of the ASTER satellite image revealed in the Oshnavieh region rock units severely disrupted by the faults and Oshnavieh is a coloured mélange. The analysis of strain geometry implies the type of tectonic setting and deformation intensity (Mookerjee and Nickleach 2011). The 3D analysis of strain ellipsoid shown on Flinn diagram, in this diagram the ratio between Ryz to Rxy define as K value (Flinn 1962). This value varied from zero to infinity. Where is the K equal to 1 the strain type is the plane strain this means the shortening in the one strain axes is equal to the elongation in the other axes and the intermediate axes are without changes. Where the k value is less than one formed in the flattening tectonic regime and strain ellipsoid is the pancake shape. This type of strain ellipsoid formed in the contractional or transpressional tectonic setting (Fossen and Cavalcante 2017; Behyari and Kanabi 2019). All samples analyzed (TS26, TS27, TS 25) from BOF shows oblate strain and revealed in this fault zone pure thrusting regime is dominated. But the samples from GTF mostly the k- values is more than one and samples located in the general constrictional zone. We proposed two scenarios for interpretation: the first is the samples (TS17, TS22, TS23) with prolate strain affected by the SBSZ but other samples far from this shear zone (TS19) deformed by oblate strain, second is the subsequent transtensional tectonic region dominated in this zone and superimposed on the previous tectonic phase. All samples were taken from shear zone located in the constrictional regime, generally the Rxy value in the KSZ is less than SBSZ (Fig 9a).

The HSU diagram applied for the 3D analyzing of the strain ellipsoid shape. In this diagram Lode's ratio (υ) calculated from the proportion of octahedral shear strain (ε) in the different strain planes. In the HSU diagram where is the Lode's ratio equal to -1 the strain ellipsoid is perfectly prolate and formed in the transpressional regime or extensional tectonic setting and where equal to 1 is perfectly oblate and deformation occurred on the contractional regime (Table. 1) (Hsu, 1966, Mookerjee and Peek, 2014). The HSU diagram indicated the Lods ratio in the shear zone sample is less than zero and octahedral shear strain (ε) in SBSZ is more than KSZ and most of samples taken from thrust zone is more than zero and deformed under flattening regime (Fig 9b).

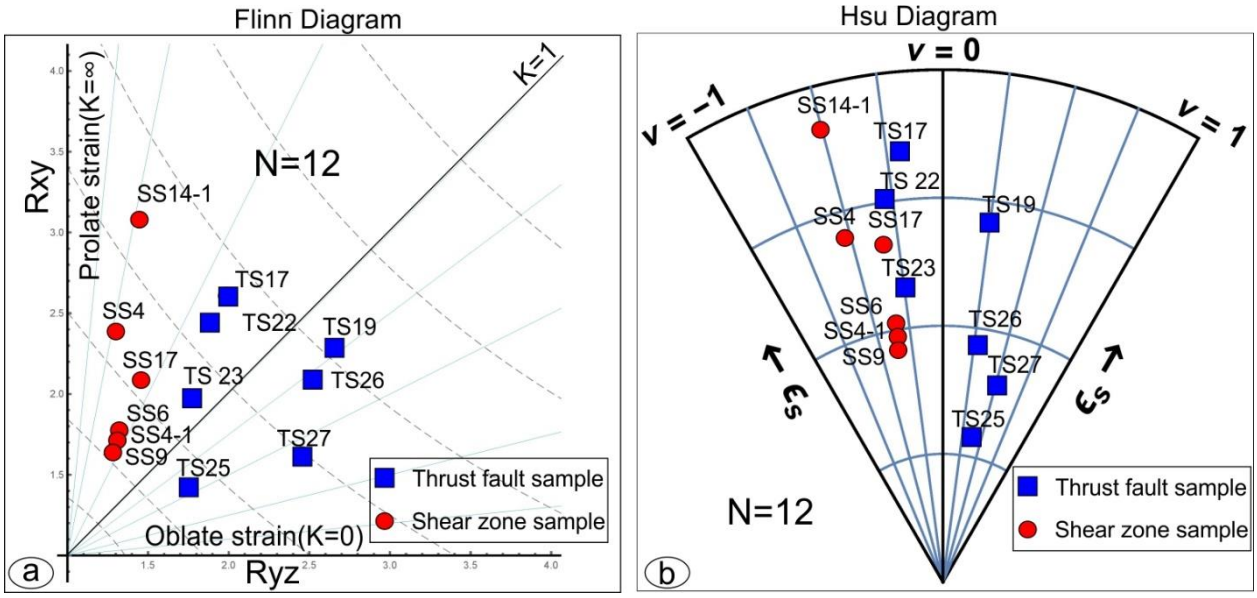


Fig 9. a) The samples plotted on the Flinn diagram b) The HSU diagram of the samples in the Study region

The contractional strain geometry of the samples that taken from fault zone, reveled in the obducted Oshnavieh ophiolite, a set of the thrust faults caused to elevated and stacking of these units and thrust them on the edge of the continental margin. The structures were located in this zone mostly deformed by the oblate strain and strain ellipsoid shape is pancake type and the k- value varied between 0.44 to 0.80 and Lods ratio 0.32 to 0.5. Structural analysis proved the dip of thrusts increasing from foreland to the hinterland. The general trend of the thrust faults is parallel with the suture zone and in the study region with the MZT. These zones mostly cut the thrust fault and strain ellipsoid is constrictional and formed under prolate strain. The k-value in the shear zone changes from 2.71 to 11.67 and Lods ratio varied between -0.42 to -0.63. The activity of the array of thrust faults and deformation in the shear zone caused the displacement of rock units and disrupted the primary sequence of the ophiolite unit in the Study region.

Table 1. The strain geometry data in the 2D and 3D form the thrust faults and shear zone of the Oshnavieh Ophiolite

| Structural position | X | Y | 2D or 3D | RXZ | RYZ | RXY | k-value | εs | Lods ratio |
|---|---|---|---|---|---|---|---|---|---|
| BOF | 494300 | 4099863 | 3D | 1.73 | 1.67 | 1.42 | 0.63 | 0.42 | 0.45 |
| BOF | 491101 | 4102234 | 3D | 2.08 | 2.53 | 2.18 | 0.77 | 0.73 | 0.32 |
| BOF | 493363 | 4101186 | 3D | 1.96 | 2.49 | 1.65 | 0.44 | 0.6 | 0.5 |
| BOF | 484516 | 4111935 | 2D | 1.87 | _ | _ | _ | _ | _ |
| GTF | 501482 | 4107914 | 2D | 1.78 | _ | _ | _ | _ | _ |
| GTF | 500027 | 4107761 | 3D | 2.17 | 1.512 | 2.558 | 3.04 | 1.1 | -0.35 |
| GTF | 495103 | 4111326 | 2D | 2.04 | _ | _ | _ | _ | _ |
| GTF | 499353 | 4106331 | 3D | 1.981 | 2.68 | 2.34 | 0.8 | 1.16 | 0.3 |
| GTF | 500019 | 4105348 | 2D | 1.9 | _ | _ | _ | _ | _ |
| GTF | 503181 | 4103270 | 2D | 1.79 | _ | _ | _ | _ | _ |
| GTF | 503813 | 4103812 | 3D | 2.1 | 1.9 | 2.43 | 1.59 | 1.31 | -0.33 |
| GTF | 504304 | 4102084 | 3D | 1.823 | 1.73 | 1.98 | 1.34 | 0.88 | -0.03 |
| GTF | 507020 | 4101780 | 2D | 1.92 | _ | _ | _ | _ | _ |
| KSZ | 500474 | 4112988 | 2D | 1.72 | _ | _ | _ | _ | _ |
| KSZ | 508588 | 4112767 | 2D | 1.85 | _ | _ | _ | _ | _ |
| KSZ | 508780 | 4112018 | 3D | 1.669 | 1.12 | 2.4 | 11.67 | 1.2 | -0.63 |
| KSZ | 508372 | 4112265 | 3D | 1.53 | 1.23 | 1.72 | 3.13 | 0.75 | -0.41 |
| KSZ | 507292 | 4111239 | 2D | 1.97 | _ | _ | _ | _ | _ |
| KSZ | 507087 | 4111265 | 3D | 1.778 | 1.31 | 1.84 | 2.71 | 0.81 | -0.42 |
| KSZ | 505726 | 4111534 | 2D | 1.71 | _ | _ | _ | _ | _ |
| KSZ | 501638 | 4112011 | 2D | 1.74 | _ | _ | _ | _ | _ |
| KSZ | 500156 | 4112988 | 3D | 2.016 | 1.18 | 1.65 | 3.61 | 0.69 | -0.42 |
| SBSZ | 508503 | 4110093 | 2D | 2.28 | _ | _ | _ | _ | _ |
| SBSZ | 507686 | 4109755 | 2D | 2.54 | _ | _ | _ | _ | _ |
| SBSZ | 505108 | 4109839 | 2D | 1.74 | _ | _ | _ | _ | _ |
| SBSZ | 503814 | 4108980 | 3D | 2.13 | 1.4 | 3.1 | 5.25 | 1.37 | -0.51 |
| SBSZ | 503559 | 4108791 | 2D | 2.66 | _ | _ | _ | _ | _ |

## 5. Conclusions:

The spectral analysis of ASTER satellite image with different band ratio combination revealed the Oshnavieh ophiolite members intensively deformed and displaced by the faulting. Best discrimination of ophiolite member provides by ((2+4)/3, (5+7)/6, (7+9)/8) band rationing also ophiolite members contact well discriminated by the principal component analysis of the (PC2, PC4 and PC 5). Structural analyses indicated the array of the thrust faults stacked ophiolite units and shear zone formed within the obducted slab. Strain ellipsoid shape analysis results show the thrust faults generally formed in the flattening conditions and compressional tectonic setting. The k- value was calculated (0.44 to 0.80) for the sample taken from the thrust fault zone. The microstructures in the shear zone and parasitic folds confirm the right-lateral shearing directions. Calculated strain ellipsoid shape samples from the shear zones revealed these zone deformed under prolate strain and constrictional tectonic regime, the k-value for these samples varied from 2.71 to 11.67. This research result indicated the oceanic crust in the Oshnavieh region is an ophiolite mélange that emplaced by the thrust fault and more deformation accommodated by the development of the shear zones.

## Acknowledgements

This work supported by the Urmia university, we are appreciated for the research office of Urmia university for assistance in conducting this research. Our gratitude is further expressed to editor, and other anonymous reviewers for reviewing our manuscript and making critical comments and valuable suggestions, which have definitely improved the quality of this work. The authors also would like express their gratitude to Peter Colman for editorial advice.

## References


Abdeen MM, Thurmond AK, Abdelsalam MG, Stern RJ (2001) Application of ASTER band-ratio images for geological mapping in arid regions: the neoproterozoic Allaqi Suture, Egypt. In: *Abstract with Program Geological Society of America* 3(3): 289.

Abrams M, Rothery D, Pontual A (1988) Mapping in the Oman ophiolite using enhanced Landsat Thematic Mapper images, *Tectonophysics* 151:387-401.

Agard P, Omrani J, Jolivet L, Mouthereau F (2005) Convergence history across Zagros (Iran): constraints from collisional and earlier deformation., *International Journal of Earth Sciences* 94:401-419.

Agard P, Omrani J, Jolivet L, Whitechurch H, Vrielynck B, Spakman W, Monié P, Meyer B, Wortel R (2011) Zagros orogeny: a subduction-dominated process, *Geological Magazine* 148:692-725.

Alavi M (1991) Sedimentary and structural characteristics of the Paleo-Tethys remnants in northeastern Iran, *The Geological Society of America Bulletin* 103:983-992.

Alavi M (1994) Tectonics of the Zagros orogenic belt of Iran: new data and interpretations, *Tectonophysics* 229:211-238.

Ali SA, Buckman S, Aswad KJ, Jones BG, Ismail SA, Nutman A (2013) The tectonic evolution of a N eo-T ethyan (E ocene–O ligocene) island-arc (W alash and N aopurdan groups) in the K urdistan region of the N ortheast Iraqi Zagros Suture Zone, *Island Arc* 22(1):104-125.

Amer R, Kusky T, Ghulam A (2010) New methods of processing ASTER data for lithological mapping: examples from Fawakhir, Central Eastern Desert of Egypt, *Journal of African Earth Sciences* 56:75-82.

Aswad KJ, Aziz NR, Koyi HAJGm (2011) Cr-spinel compositions in serpentinites and their implications for the petrotectonic history of the Zagros Suture Zone, Kurdistan Region, Iraq, *Geological magazine* 148:802-818.

Axen GJ, Lam PS, Grove M, Stockli DF, Hassanzadeh J (2001) Exhumation of the west-central Alborz Mountains, Iran, Caspian subsidence, and collision-related tectonics, *Geology* 29:559-562.

Babaie HA, Babaei A, Ghazi AM, Arvin M (2006) Geochemical, 40Ar/39Ar age, and isotopic data for crustal rocks of the Neyriz ophiolite, Iran, *Canadian Journal of Earth Sciences* 43:57-70.

Ballato P, Uba CE, Landgraf A, Strecker MR, Sudo M, Stockli DF, Friedrich A, Tabatabaei SH (2010) Arabia-Eurasia continental collision: Insights from late Tertiary foreland-basin evolution in the Alborz Mountains, northern Iran, *Geological Society of America Bulletin* 123:106-131.

Behyari M, Kanabi A (2019) Constraining of strain ellipsoid shape from sectional data in the au bearing shear zone west of Iran, *Acta Geodynamica et Geromaterialia* 16:131-143.

Behyari M, Mohajjel M, Sobel ER, Rezaeian M, Moayyed M, Schmidt A (2017) Analysis of exhumation history in Misho Mountains, NW Iran: Insights from structural and apatite fission track data, *Neues Jahrbuch für Geologie und Paläontologie-Abhandlungen* 283:291-308.

Behyari M, Nouraliee J, Ebrahimi DJAGSEE (2018) Structural Control on the Salmas Geothermal Region, Northwest Iran, from Fractal Analysis and Paleostress Data, . *Acta Geologica Sinica-English Editio* 92:1728-1738.

Behyari M, Shahbazi M (2019) Strain and vorticity analysis in the Zagros suture zone (W Iran): Implications for Neo-Tethys post-collision events, *Journal of Structural Geology* 126:198-209.

Berberian M, King G (1981) Towards a paleogeography and tectonic evolution of Iran, *Canadian journal of earth sciences* 5:101-117.

Bhattacharyya P, Hudleston P (2001) Strain in ductile shear zones in the Caledonides of northern Sweden: a three-dimensional puzzle, *Journal of Structural Geology* 23:1549-1565.

Cloutis EA, Sunshine J, Morris R (2004) Spectral reflectance-compositional properties of spinels and chromites: Implications for planetary remote sensing and geothermometry, *Meteoritics & Planetary Science* 39:545-565.

Flinn D (1962) On folding during three-dimensional progressive deformation, *Quarterly Journal of the Geological Society* 118:385-428.

Fossen H, Cavalcante G (2017) Shear zones–A review, *Earth-Science Reviews* 171:434-455.

François T, Agard P, Bernet B, Meyer B, Chung S-L, Zarrinkoub MH, Burov E, Monié P (2014) Cenozoic exhumation of the internal Zagros: first constraints from low-temperature thermochronology and implications for the build-up of the Iranian plateau, *Lithos* 206-207:100-112.

Hassanipak A, Ghazi A (2000) Petrology, geochemistry and tectonic setting of the Khoy ophiolite, northwest Iran: implications for Tethyan tectonics, *Journal of Asian Earth Sciences* 18:109-121.

Hunt GR, Salisbury JW, Lenhoff CJ (1974) Visible and near infrared spectra of minerals and rocks: IX. Basic and ultrabasic igneous rocks, *Modern Geology* 5:15-22.

Keshavarz S, Faghih A (2020) Heterogeneous sub-simple deformation in the Gol-e-Gohar shear zone (Zagros, SW Iran): insights from microstructural and crystal fabric analyses, *International Journal of Earth Sciences* 109:421-438.

Khalatbari-Jafari M, Juteau T, Bellon H, Emami H (2003) Discovery of two ophiolite complexes of different ages in the Khoy area (NW Iran), *Comptes Rendus Geoscience* 335:917-929.

Khalatbari-Jafari M, Juteau T, Bellon H, Whitechurch H, Cotten J, Emami H (2004) New geological, geochronological and geochemical investigations on

the Khoy ophiolites and related formations, NW Iran, *Journal of Asian Earth Sciences* 23:507-535.

Lisle RJ (2010) Strain analysis from point fabric patterns: An objective variant of the Fry method, *Journal of Structural Geology* 32:975-981.

Mahdavi M, Dabiri R, Hosseini ES (2015) Magmatic evolution and compositional characteristics of tertiary volcanic rocks associated with the Venarch manganese mineralization, SW Qom, central Iran. *Earth Sciences Research Journal* 19(2):141-5.

Moghadam HS, Stern RJ. (2015) Ophiolites of Iran: Keys to understanding the tectonic evolution of SW Asia:(II) Mesozoic ophiolites, *Journal of Asian Earth Sciences* 100:31-59.

Mohajjel M, Fergusson C, Sahandi M (2003) Cretaceous–Tertiary convergence and continental collision, Sanandaj–Sirjan zone, western Iran, *Journal of Asian Earth Sciences* 21:397-412.

Mohajjel M, Fergusson CL (2000) Dextral transpression in Late Cretaceous continental collision, Sanandaj–Sirjan zone, western Iran, *Journal of structural geology* 22:1125-1139.

Monsef I, Rahgoshay M, Mohajjel M, Moghadam HS. (2010) Peridotites from the Khoy Ophiolitic Complex, NW Iran: Evidence of mantle dynamics in a supra-subduction-zone context, *Journal of Asian Earth Sciences* 38:105-120.

Mookerjee M, Fortescue FQ (2016) Quantifying thinning and extrusion associated with an oblique subduction zone: An example from the Rosy Finch Shear Zone, *Tectonophysics* 693:290-303.

Mookerjee M, Nickleach S (2011) Three-dimensional strain analysis using Mathematica, *Journal of Structural Geology* 33:1467-1476.

Passchier CW, Trouw RA (1996) Microtectonics vol 2. *Springer*.

Rajendran S, Al-Khirbash S, Pracejus B, Nasir S, Al-Abri AH, Kusky TM, Ghulam A (2012) ASTER detection of chromite bearing mineralized zones in Semail Ophiolite Massifs of the northern Oman Mountains: Exploration strategy, *Ore geology reviews* 44:121-135.

Ramsay J, Graham R (1970) Strain variation in shear belts, *Canadian Journal of Earth Sciences* 7:786-813.

Ring U, Bernet M, Tulloch A (2015) Kinematic, finite strain and vorticity analysis of the Sisters shear zone, Stewart Island, New Zealand, *Journal of Structural Geology* 73:114-129.

Rowan LC, Hook SJ, Abrams MJ, Mars JC (2003) Mapping hydrothermally altered rocks at Cuprite, Nevada, using the Advanced Spaceborne Thermal Emission and Reflection Radiometer (ASTER), a new satellite-imaging system, *Economic Geology* 98:1019-1027.

Saccani E, Allahyari K, Beccaluva L, Bianchini G. (2013) Geochemistry and petrology of the Kermanshah ophiolites (Iran): Implication for the interaction between passive rifting, oceanic accretion, and OIB-type components in the Southern Neo-Tethys Ocean, *Gondwana Research* 24:392-411.

Saccani E, Allahyari K, Rahimzadeh B (2014) Petrology and geochemistry of mafic magmatic rocks from the Sarve-Abad ophiolites (Kurdistan region, Iran): Evidence for interaction between MORB-type asthenosphere and OIB-type components in the southern Neo-Tethys Ocean, *Tectonophysics* 621:132-147.

Sarem MN, Abedini MV, Dabiri R, Ansari MR (2021) Geochemistry and petrogenesis of basic Paleogene volcanic rocks in Alamut region, Alborz mountain, north of Iran. *Earth Sciences Research Journal* 25(2):237-45.

Sarkarinejad K (2007) Quantitative finite strain and kinematic flow analyses along the Zagros transpression zone, Iran, *Tectonophysics* 442:49-65.

Sarkarinejad K, Faghih A, Grasemann B (2008) Transpressional deformations within the Sanandaj–Sirjan metamorphic belt (Zagros Mountains, Iran), *Journal of Structural Geology* 30:818-826.

Sarkarinejad K, Godin L, Faghih A (2009) Kinematic vorticity flow analysis and 40Ar/39Ar geochronology related to inclined extrusion of the HP–LT metamorphic rocks along the Zagros accretionary prism, Iran, *Journal of Structural Geology* 31:691-706.

Shafaii Moghadam H, Stern RJ (2011) Geodynamic evolution of Upper Cretaceous Zagros ophiolites: formation of oceanic lithosphere above a nascent subduction zone, *Geological Magazine* 148:762-801.

Shahabpour J (2005) Tectonic evolution of the orogenic belt in the region located between Kerman and Neyriz, *Journal of Asian Earth Sciences* 24:405-417.

Stallard A, Shelley D (1995) Quartz c-axes parallel to stretching directions in very low-grade metamorphic rocks, *Tectonophysics* 249:31-40.

Tangestani MH, Jaffari L, Vincent RK, Sridhar BM (2011) Spectral characterization and ASTER-based lithological mapping of an ophiolite complex: A case study from Neyriz ophiolite, SW Iran, *Remote Sensing of Environment* 115:2243-2254.

Vitale S, Mazzoli S (2010) Strain analysis of heterogeneous ductile shear zones based on the attitudes of planar markers, *Journal of Structural Geology* 32:321-329.

Watts M, Williams G (1983) Strain geometry, microstructure and mineral chemistry in metagabbro shear zones: a study of softening mechanisms during progressive mylonitization, *Journal of Structural Geology* 5:507-517.

Yazdi A, Ashja Ardalan A, Emami MH, Dabiri R, Foudazi M (2019) Magmatic interactions as recorded in plagioclase phenocrysts of quaternary volcanics in SE Bam (SE Iran). *Iranian Journal of Earth Sciences* 11(3):215-25.